Journal of Engineering Mathematics **42:** 225–242, 2002.

Exact solutions for the viscous sintering of multiply-connected fluid domains

DARREN CROWDY
Department of Mathematics, Imperial College of Science, Technology and Medicine, 180 Queen's Gate, London, SW7 2BZ, U.K. Email: d.crowdy@ic.ac.uk

Received 10 September 2001; accepted in revised form 31 January 2002

Abstract. Exact solutions for the viscous sintering of multiply-connected fluid domains are found. The approach is based on a recent observation by the author connecting viscous sintering and quadrature identities. The solutions are exact in that the evolution can be described in terms of a finite set of time-dependent parameters; it is shown that the evolution of certain initial fluid domains under the equations of Stokes flow driven by surface tension can be calculated by following the evolution of the coefficients of an algebraic curve. These coefficients satisfy a finite system of first-order nonlinear ordinary differential equations. Practical methods for solving this system are described. By way of example, explicit calculations of the sintering of unit cells deriving from square packings involving both unimodal and bimodal distributions of particles are given.

Key words: algebraic curves, multiply-connected, viscous sintering.

1. Introduction

Sintering is a process by which a granular compact of particles (*e.g.* metal or glass) is raised to a sufficiently high temperature that the individual particles become mobile and release surface energy in such a way as to produce inter-particulate bonds [1]. At the start of a sinter process, any two particles which are initially touching develop a thin neck which, as time evolves, grows in size to form a more developed bond. As the necks grow in size, the sinter body densifies and any enclosed pores between particles eventually close up. The macroscopic material properties of the compact at the end of the sinter process depend heavily on the degree of densification. In industrial application, it is crucial to be able to obtain accurate and reliable estimates of the time taken for pores to close (or reduce to a sufficiently small size) within any given initial sinter body in order that industrial sinter times are optimized without compromising the macroscopic properties of the final densified material.

In order to model the sintering process theoretically so that quantitative predictions can be made, it is usual to divide the process into three stages; the *initial, intermediate* and *final* stage. Models have been devised to study each stage of the process. In such models, the state of the sinter kinetics is typically described by isolating a geometrical unit cell and studying a 'unit problem'. An important *initial* stage model is the two-sphere model due to Frenkel [2]. Frenkel made some major simplifications regarding the flow field in order to deduce an equation governing the neck-growth rate between two initially-touching spheres as they coalesce. This is done using an energy principle which equates the viscous-flow dissipation with the rate at which surface energy is released. Scherer [1] introduced an *intermediate* stage model (the 'cylinder model') in which the densifying material is modelled by an idealized cubic array of intersecting cylinders getting gradually shorter and thicker. Mackenzie and

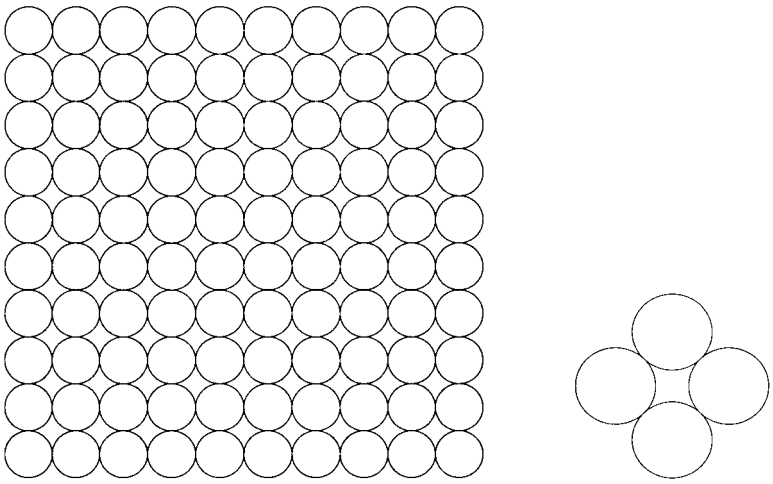

Figure 1. Sinter compact with regular square packing of equal particles. Natural choice of square unit cell is shown to the right. Unit cell has just one enclosed pore.

Shuttleworth [3] presented a final stage model comprising spherical pores in a fluid/solid matrix.

In the case of planar sintering the analogue of Frenkel's two-sphere unit problem is the coalescence of two equal cylindrical particles. Remarkably, Hopper [4],[5] analysed this unit problem and showed that it admits exact solutions in the sense that the free-boundary problem can be reduced to tracking the evolution of just two real parameters in a conformal map. In a natural generalization of Hopper's result, Richardson [6] found an exact solution for the coalescence of two unequal cylinders. Many related results have followed and Howison [7] has compiled a comprehensive list of references concerned with this problem. In respect of exact solutions for multiply-connected fluid domains, Crowdy and Tanveer [8], Richardson [9] and Crowdy [10] have independently found and studied (using different, but related, approaches) exact conformal-mapping solutions in the case of *doubly*-connected fluid domains but, beyond that, no exact solutions for fluid regions of higher connectivity appear to exist in the literature. This paper presents a general method for identifying and constructing exact solutions for fluid domains of arbitrary finite connectivity.

To motivate our interest in multiply-connected fluid domains, consider the unit problem shown in Figure 1 comprising four equal cylinders forming a square unit cell for the extended packing also depicted. During the early stages of sintering, this configuration will form a doubly-connected fluid region with a single enclosed pore which eventually closes up. Van der Vorst [11] has shown numerically that Hopper's solution for the coalescence of just two equal isolated particles provides an excellent description for the early stage neck-growth in this more complicated doubly-connected unit problem. (This fact has also been corroborated by Crowdy [10] by studying exact conformal-map solutions.) An advantage of Hopper's solution is its mathematical simplicity; a drawback is that the fluid region is simply-connected with no shrinking pores so that while the initial stage neck-growth is captured, it is difficult to infer accurate estimates of pore-shrinkage times. Van der Vorst [11] estimated the shrinkage time numerically. Since then, exact conformal-mapping solutions for this unit problem have been developed [8] [9] [10] which provide an alternative method of calculating the pore-shrinkage times.

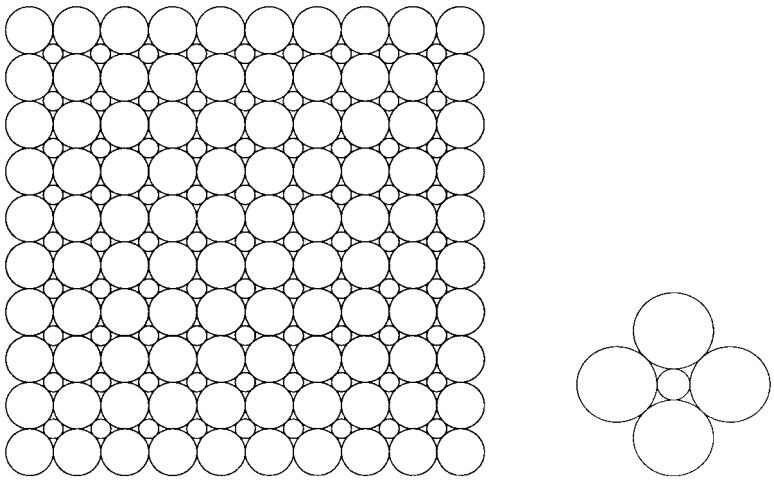

Figure 2. Sinter compact with regular square packing as in Figure 1 but with small interstitial particles invading the pores. Natural choice of square unit cell is shown to the right. Unit cell has four enclosed pores.

Now consider the packing of Figure 2 which might arise physically when smaller interstitial particles are introduced in the unimodal compact of Figure 1. A natural choice of unit problem (or unit cell) in this case is also shown in Figure 2 and consists of a small particle filling the hole formed by an annular configuration of four larger ones. This unit problem is interesting for two reasons. First, it possesses two distinct types of neck region, *viz.* four necks between particles of equal size, and four necks between unequal particles. Second, under the sinter dynamics the fluid domain will become quintuply-connected (at least, until the pores shrink away). No exact conformal-mapping solutions to this problem have yet been constructed. Suppose that one attempts to estimate densification rates based on the neck-growth rates of exact *simply*-connected unit problems; should one use Hopper's exact solution for the coalescence of *equal* particles, or Richardson's result for *unequal* particles? A combination of the two seems more appropriate, but how to combine them? Furthermore, even if these two unit problems could be appropriately combined, how to infer estimates of pore-shrinkage times? What is ideally needed is a full resolution of the sinter dynamics of the unit problem in Figure 2 which shares the benefits of exactness of Hopper's solution. Failing that, a full numerical simulation will have to be used. Of course, the unit problem in Figure 2 cannot be expected to resolve pore-shrinkage rates with complete accuracy because it is studied in isolation and not as part of the full doubly-infinite lattice. Nevertheless, it is reasonable to suggest that, in contrast to the simply-connected unit problems just mentioned, the unit problem in Figure 2 will provide a good first approximant to the pore-shrinkage times, especially if the pore sizes are small compared to the area of fluid in the unit cell (so that the effect of neighbouring units is not large). On this point, it is worth remarking that the idea of modelling pore shrinkage by isolating a single unit cell and approximating the mean effect of all other pores in a compact by a uniform-pressure ambient region has been used before in phenomenological models of sintering [3]. Van der Vorst [13] considered the effect of the doubly-infinite lattice using numerical boundary-element methods.

The principal new result of this paper is to show that the coalescence of the unit problem in Figure 2 in fact admits an exact solution, in exactly the same spirit as Hopper's classic result, and that its evolution can be reduced to tracking just five real parameters. A second new feature

is our approach. Almost invariably, studies in the literature (see [7]) involving exact solutions to planar sintering problems rely on conformal-mapping theory. The use of conformal maps to parametrize the fluid boundaries is a matter of choice; it will be seen here that there is an alternative, equally effective, way to follow the free boundaries. By exploiting ideas connecting viscous sintering with quadrature identities recently expounded by the present author [12], sintering is described here by following the evolution of an algebraic curve.

2. The viscous-sintering model

Consider the quasi-steady evolution of an M-connected plane blob of very viscous (Stokes) fluid evolving purely under the effects of surface tension. If a stream function $\psi(x, y)$ is introduced, so that the fluid velocity field $\mathbf{u}$ is given by

$$\mathbf{u} = (\psi_y, -\psi_x), \tag{1}$$

then, it is well-known [14] that

$$\nabla^4 \psi = 0 \quad \text{in } D(t). \tag{2}$$

On the blob boundary the stress condition is

$$-pn_j + 2e_{jk}n_k = \kappa n_j, \tag{3}$$

where κ is the surface curvature, p the fluid pressure and e_{jk} the usual rate-of-strain tensor; $\mathbf{n}$ is the normal to the surface. The kinematic condition is that

$$\mathbf{u}.\mathbf{n} = V_n, \tag{4}$$

at each point on the interface, where V_n is the normal velocity of the interface. In what follows, the same non-dimensionalization of physical variables as used in [14] is employed.

The general solution of (2) at each instant can be written as

$$\psi = \mathfrak{Im}[\bar{z} f(z, t) + g(z, t)], \tag{5}$$

where the *Goursat functions* $f(z, t)$ and $g(z, t)$ are analytic everywhere in the fluid region $D(t)$ and $z = x + \mathrm{i}y$ is the usual complex variable; $f(z, t)$ must also be single-valued if there are no net forces on the fluid blob; $g(z, t)$ need not be single-valued and, in the present application, one expects the presence of logarithmic singularities of $g(z, t)$ corresponding to sources or sinks in the enclosed pores: See Richardson [15], [9] for a further discussion of these points. The following relations can easily be established:

$$\begin{aligned} p &= \mathfrak{Re}[4f'(z, t)], \\ u + \mathrm{i}v &= -f(z, t) + z\bar{f}'(\bar{z}, t) + \bar{g}'(\bar{z}, t), \\ e_{11} + \mathrm{i}e_{12} &= z\bar{f}''(\bar{z}, t) + \bar{g}''(\bar{z}, t). \end{aligned} \tag{6}$$

where primes denote differentiation with respect to the first argument of the function. Conjugate functions such as $\bar{f}$ and $\bar{g}$ are defined via $\bar{f}(z) = \overline{f(\bar{z})}$. Let the M-connected fluid domain have boundary $\partial D(t)$ consisting of an outermost boundary $\partial D_0(t)$ with $M-1$ enclosed boundaries $\partial D_i(t), i = 1, \ldots, M-1$. Defining s to be the arclength traversed in an anticlockwise direction on $\partial D_0(t)$ and in a clockwise direction around $\partial D_i(t), i = 1, \ldots, M-1$, it can be shown [14] that the stress boundary conditions on $\partial D(t)$ can be written in the form

$$f(z,t) + z\bar{f}'(\bar{z},t) + \bar{g}'(\bar{z},t) = \mathrm{i}\frac{z_s}{2} + C_i(t), \quad \text{on } \partial D_i(t), \quad i = 0, 1, \ldots, M-1, \quad (7)$$

where $C_i(t)$ are constants of integration. At each instant, the domain and conditions (7) determine $f(z,t)$, $g(z,t)$ and the constants $C_i(t)$. It can be assumed, without loss of generality, that $C_0(t) = 0$. The kinematic condition on $\partial D(t)$ can be written as

$$\mathfrak{Im}[(z_t - (u + \mathrm{i}v))\bar{z}_s] = 0, \quad (8)$$

and, in this quasi-steady model, is the equation governing the subsequent evolution of the boundary.

3. Quadrature domains

The simplest example of a quadrature domain [16] is a circular disk. For a disk D of radius r centred at the origin, the *mean value formula* states that

$$\int\int_D h(z)\,\mathrm{d}x\,\mathrm{d}y = \pi r^2 h(0), \quad (9)$$

where $h(z)$ is an arbitrary function analytic in the disk and integrable over it (in the sense of area measure).

More generally, a domain D is called a *quadrature domain* [16] if the following *quadrature identity* holds for all integrable analytic $h(z)$ in D:

$$\int\int_D h(z)\,\mathrm{d}x\,\mathrm{d}y = \sum_{k=1}^{m}\sum_{j=0}^{n_{k-1}} c_{kj} h^{(j)}(z_k), \quad (10)$$

for some set of coefficients $\{c_{kj}\}$ and same point set $\{z_k\}$. Here $h^{(j)}(z)$ denotes the jth derivative of $h(z)$. The complex numbers $\{c_{kj}\}$ and $\{z_k\}$ are called the *quadrature data* of D.

4. Algebraic curves

It is known [16] that, if D is a quadrature domain satisfying some identity (10) then its boundary ∂D is an *algebraic curve* given, to within a finite set of *special points* V_0, by

$$\partial D = \{z \in \mathbb{C} | \mathcal{P}(z,\bar{z}) = O\} \Big\backslash V_0, \quad (11)$$

where

$$\mathcal{P}(z,w) = \sum_{k,j=0}^{n} a_{kj} z^k w^j, \quad (12)$$

where $n = \sum_{k=1}^{m} n_k$ is referred to as the *order* of the quadrature identity, and where the coefficients $\{a_{kj}\}$ satisfy the hermitian property

$$\bar{a}_{jk} = a_{kj}. \quad (13)$$

The matrix of coefficients $\{a_{kj}\}$ will henceforth be referred to as the $((n+1)$-by-$(n+1))$ matrix $\mathbf{A}$. The set V_0 is a set of *isolated* points in D at which

$$\mathcal{P} = \frac{\partial \mathcal{P}}{\partial z} = 0. \tag{14}$$

An alternative way of writing (12) is in the form

$$\mathcal{P}(z, w) = \sum_{j=0}^{n} w^j P_j(z), \tag{15}$$

where $P_j(z)$ is a polynomial (in z) of degree at most n. There is a normalization degree of freedom in the specification of $\mathcal{P}(z, w)$ which is set by insisting that $a_{nn} = 1$.

It is natural to expect there must be some connection between the quadrature data $\{c_{kj}, z_k\}$ and the set of coefficients $\{a_{kj}\}$ defining the associated algebraic curve. Indeed, there is a *partial* connection embodied in the following theorem of Gustafsson [17]:

THEOREM 4.1.

For a quadrature domain satisfying the quadrature identity (10) of order n, the identity

$$\frac{1}{\pi} \sum_{k=1}^{m} \sum_{j=0}^{n_k - 1} \frac{j! c_{kj}}{(z - z_k)^{j+1}} \equiv a_{nn-1} - \frac{P_{n-1}(z)}{P_n(z)}, \tag{16}$$

where

$$P_{n-1}(z) = a_{n,n-1} z^n + a_{n-1,n-1} z^{n-1} + \cdots + a_{0,n-1}, \tag{17}$$

$$P_n(z) = z^n + a_{n-1,n} z^{n-1} + \cdots + a_{0,n}, \tag{18}$$

sets up a one-to-one correspondence between the set of coefficients $\{c_{kj}, z_k\}$ and the last two columns (and rows) of the coefficient matrix **A**.

5. Viscous sintering and quadrature domains

Crowdy [12] has shown that, in the case of a simply-connected fluid region, the dynamics of viscous sintering is such as to preserve quadrature identities. Thus, if an initial blob of fluid is a quadrature domain with a given associated quadrature identity, the fluid blob *remains* a quadrature domain under evolution (at least, for sufficiently short times), its associated quadrature identity evolving in time according to the dynamics of the viscous-sintering problem. The analysis in [12] establishes this fact using the (complexified) equations of motion of Section 2 and without the introduction of conformal maps at any stage. The analysis of Crowdy [12] forms the basis for the mathematical approach to viscous sintering developed here and underlies the proof of the following theorem.

THEOREM 5.1.

Provide an initial M-connected fluid domain (with analytic boundary) is such that

(i) *it is a quadrature domain,*

(ii) *it is such that the constants of integration $C_i(t), i = 0, \ldots, M-1$ can consistently be assumed equal to zero throughout the evolution, and assuming the evolution is locally analytic in time then, at least for short enough times, its evolution under the dynamics of viscous sintering is such that it remains a quadrature domain of the same order.*

Proof: By inspection of the theorems established in Crowdy [12] for the case of a simply-connected fluid region in which $\partial D(t)$ consists of just one component, it is clear that if $h(z, t)$ (in the notation of [12]) is assumed to be a single-valued analytic integrable function in the (now) multiply-connected domain $D(t)$, the only way in which the proofs would differ is if any of the constants $C_i(t)$ arising in the integrated stress conditions on any of the component curves $\partial D_i(t)$ of $\partial D(t)$ is non-zero or if either $f(z, t)$ or $g'(z, t)$ is not single-valued in $D(t)$. Therefore, under assumption (ii) that $C_i(t) = 0, i = 0, \ldots, M-1$, all the theorems in [12] establishing the preservation of quadrature domains still hold for multiply-connected fluid regions, and constitute a proof of Theorem 5.1. The qualification 'for short enough times' is inherited from the proofs of [12] which assume that the dynamics is locally analytic in time for some $0 \leq t < T$ where T is non-zero.

An alternative proof of Theorem 5.1 can be constructed based on a formulation of the viscous-sintering problem in terms of Cauchy transforms of the domain as formulated (in the case of simply-connected domains) by Crowdy [18].

It remains to determine in which circumstances all constants $C_i(t)$ can consistently be assumed equal to zero under evolution. This result is due to Richardson [9] who discusses doubly-connected fluid domains. The constants $C_i(t)$ are determined instantaneously by the domain itself. In a doubly-connected fluid domain there would be two such constants, $C_0(t)$ and $C_1(t)$. By transformations of the integrated stress conditions on each boundary, Richardson [9] finds that, if the domain is invariant to rotations about the origin by an angle which is not an integral multiple of 2π, then $C_0(t) = C_1(t) = 0$. This argument also applies to rotationally-symmetric domains of higher connectivity. Consider a transformation $(z, f, g, \{C_i\}) \mapsto (\mathcal{Z}, \mathcal{F}, \mathcal{G}, \{\mathcal{C}_i\})$ (where $i = 0, 1, \ldots, M-1$) corresponding to a rotation of the flow domain about the origin through an angle θ (which is not an integral multiple of 2π). Inspection of the formula in (6) for the velocity field implies that we must have

$$\mathcal{Z} = z\mathrm{e}^{\mathrm{i}\theta}, \quad \mathcal{F}(\mathcal{Z}) = f(z)\mathrm{e}^{\mathrm{i}\theta}, \quad \mathcal{G}'(\mathcal{Z}) = g'(z)\mathrm{e}^{-\mathrm{i}\theta}. \tag{19}$$

By using (19) in the stress condition we have that the constants C_i transform as

$$\mathcal{C}_i = C_i\mathrm{e}^{\mathrm{i}\theta}. \tag{20}$$

However, if the domain is invariant under a rotation through θ then, in order that the stress boundary conditions be similarly invariant, we must have $C_i = 0$. We therefore restrict attention to initial multiply-connected quadrature domains with such a rotational symmetry about the origin so that condition (ii) in the statement of Theorem 5.1 holds. Such initial domains will then evolve in time as quadrature domains.

6. Hopper's example: two coalescing particles

Hopper's exact solution for the coalesence of two equal particles can be understood from exactly this perspective. Hopper himself [4], [5] did not use such a perspective but instead derived his result based on analysis performed in a parametric ζ-plane. Hopper describes the free-boundary evolution using a conformal map $z(\zeta, t)$ from a unit ζ-circle to the fluid domain $D(t)$. The map has the form

$$z(\zeta, t) = \frac{R(t)\zeta}{\zeta^2 - a^2(t)}, \tag{21}$$

where $R(t)$ and $a(t)$ are two real time-evolving parameters for which Hopper gives the appropriate evolution equations.

There is an alternative way to describe this evolution. Let $D(t)$ be Hopper's fluid region at time t. By Green's theorem,

$$\int\int_{D(t)} h(z)\,\mathrm{d}x\,\mathrm{d}y = \frac{1}{2\mathrm{i}}\oint_{\partial D(t)} h(z)\bar{z}\,\mathrm{d}z, \tag{22}$$

where $h(z)$ is some integrable analytic function over $D(t)$. Using the conformal map (21) and the residue theorem,

$$\int\int_{D(t)} h(z)\,\mathrm{d}x\,\mathrm{d}y = \frac{1}{2i}\oint_{|\zeta|=1} h(z)\bar{z}z_\zeta\,\mathrm{d}\zeta = \pi r^2(t)h(z_a(t)) + \pi r^2(t)h(-z_a(t)), \tag{23}$$

where

$$z_a(t) = z(a^{-1}, t), \qquad r^2(t) = -\frac{R(t)z_\zeta(a^{-1}, t)}{2a^2(t)}. \tag{24}$$

we find that (23) is a quadrature identity. Hopper's fluid regions $D(t)$ are therefore quadrature domains. Equation (24) provides relations between the conformal-map parameters $\{R(t), a(t)\}$ and the quadrature data $\{r(t), z_a(t)\}$. By the results of Section 4, the fluid boundary $\partial D(t)$ must therefore be given (to within some finite set $V_0(t)$ which must now be assumed to evolve in time) by some algebraic curve $\mathcal{P}(z, \bar{z}; t) = 0$. In what follows, for brevity, parameters such as $z_a(t)$ which are functions of time will simply be written z_a.

The algebraic curve corresponding to Hopper's initial condition of two equal touching circular disks is trivial to find. If the centres of the disks are at $\pm z_a$ and their point of contact is the origin, then

$$P(z, \bar{z}) = (|z - z_a|^2 - z_a^2)(|z + z_a|^2 - z_a^2) = z^2\bar{z}^2 - z_a^2 z^2 - z_a^2\bar{z}^2 - 2z_a^2 z\bar{z} = 0. \tag{25}$$

By Theorem 5.1 (or the results of [12]) it is known that the domain continues to satisfy a quadrature identity of the form (23) under evolution. The boundary therefore remains an algebraic curve. The order of the quadrature identity is 2; the algebraic curve matrix $\mathbf{A}(t)$ is therefore 3-by-3. Theorem 4.1 and (23) can be used to deduce the last two rows (and columns) of $\mathbf{A}(t)$:

$$\mathbf{A}(t) = \begin{pmatrix} e & 0 & -z_a^2 \\ 0 & -2r^2 & 0 \\ -z_a^2 & 0 & 1 \end{pmatrix}, \tag{26}$$

so that the algebraic curve is

$$z^2\bar{z}^2 - z_a^2\bar{z}^2 - z_a^2\bar{z}^2 - 2r^2 z\bar{z} + e = 0. \tag{27}$$

Once the matrix $\mathbf{A}(t)$ is found, the non-isolated solutions of (27) provide a closed-form algebraic representation of the fluid boundary that is easily plotted using standard graphics packages. It rivals (21) as a means of describing the boundary evolution in terms of a finite set of parameters.

If (23) and (26) are compared it is clear that some of the coefficients of $\mathbf{A}(t)$ depend explicitly on the quadrature data. It is therefore necessary to find ordinary differential equations for the quadrature data. Such equations were derived in Crowdy [12]. Example 1 of [12] considers an (order 3) quadrature identity of a form analogous to (23). By adapting this example, we deduce that

$$\dot{r}(t) = 0, \qquad \dot{z}_a(t) = -2f(z_a, t), \tag{28}$$

where $f(z,t)$ is the Goursat function introduced in Section 2. Thus, $r(t)$ is a conserved quantity. To determine $f(z_a,t)$, we propose use of the *Sherman-Lauricella integral equation*. This is described in the next section.

It only remains to find e which is apparently not determined in any explicit way by the quadrature data. Crowdy [19] has recently considered the general problem of reconstructing a quadrature domain from its quadrature identity using algebraic curves. One way to determine e is to consider the equation

$$\mathcal{F}(e) = 0. \tag{29}$$

where

$$\mathcal{F}(e) \equiv \frac{1}{2\mathrm{i}} \oint_{\partial D(t)} \bar{z}\mathrm{d}z - 2\pi r^2. \tag{30}$$

This is simply the area relation for the quadrature domain and is obtained by taking $h(z) = 1$ in the quadrature identity and using Green's theorem to convert the area integral to a line integral. Note that $\mathcal{F}$ depends on e because the line integral is taken around the algebraic curve ∂D whose definition contains e. Equation (29) can be solved for e at each instant by using a form of Newton's method which iterates on the algebraic curve. Note that it requires $\mathcal{O}(N)$ operations to evaluate $\mathcal{F}(e)$ in a numerical quadrature. In this case, the solution is $e(t) = 0$.

Finally we remark that, in this particular case, it is not strictly necessary to solve (29) for e. It turns out that there is a simpler way to determine that $e(t) = 0$ based on some additional analytical structure of quadrature domains, *i.e.* consideration of the *special point* set V_0. Such considerations are useful whenever the domains of interest have sufficient symmetry. We refer the reader to Crowdy [19] for more details and additional examples.

6.1. Sherman–Lauricella integral equation

In Hopper's evolution equations, the evolution of $a(t)$ depends on a non-local quantity which requires a (numerical) integration around the entire fluid boundary for its determination. This requires $\mathcal{O}(N)$ operations where N is the number of points in the discretization of the boundary ∂D. The analogous non-local quantity in the algebraic curve formulation above is $f(z_a(t),t)$. To determine it, we write $f(z,t)$ as a Cauchy integral

$$f(z,t) = \frac{1}{2\pi\mathrm{i}} \oint_{\partial D(t)} \frac{\omega(\eta,t)}{\eta - z}\mathrm{d}\eta, \tag{31}$$

(with a similar expression for $g'(z,t)$ - see [20] [21] for details). The Sherman-Lauricella equation for the density $\omega(z,t)$ is

$$\omega(z,t) + \frac{1}{2\pi\mathrm{i}} \oint_{\partial D(t)} \omega(\eta,t)\mathrm{d}\log\left(\frac{\eta - z}{\bar{\eta} - \bar{z}}\right) - \frac{1}{2\pi\mathrm{i}} \oint_{\partial D(t)} \overline{\omega(\eta,t)}\mathrm{d}\left(\frac{\eta - z}{\bar{\eta} - \bar{z}}\right) = -\mathrm{i}\frac{z_s}{2}. \tag{32}$$

This integral equation has a number of advantageous features. First, the kernels $\mathrm{d}\log((\eta - z)/(\bar{\eta} - \bar{z}))$ and $\mathrm{d}((\eta - z)/(\bar{\eta} - \bar{z}))$ are continuous along each component of the curve $\partial D(t)$ so that (32) is a second-kind integral equation with smooth kernel; second, the Sherman–Lauricella equation (S–L equation) extends readily [21] to the case of multiply-connected fluid domains

which are of interest here; third, very recent research has shown that Fast Multipole Methods [21] can be applied to solve the S–L equation (in large-scale multiply-connected domains) in $\mathcal{O}(N)$ operations which is significant in that it renders the algebraic curve approach in the present application numerically competitive with the conformal-mapping approach.

Greengard *et al.* [21] present a numerical method for the solution of the S–L equation in a multiply-connected domain. Their formulation relies on finding N_i points, equally-spaced with respect to some parametrization, on each component curve ∂D_i. For an M-connected domain, there will be a total of $N \equiv \sum_{i=0}^{M-1} N_i$ points on $\partial D(t)$. The aim is to determine the value of the density function $\omega_k, k = 1, \ldots, N$ at this set of points. The S–L equation is then discretized using the trapezoidal rule which gives superalgebraic convergence for smooth data on smooth boundaries. In the present application, a formula for the algebraic curve is known at each instant which can readily be used to find a resampling of the boundary points equally-spaced with respect to the arclength parameter s introduced earlier. Greengard *et al.* [21] use Fast Multipole Methods (FMM) to invert the resulting matrix equation for the vector ω_i in $\mathcal{O}(N)$ operations; here, for the purposes of a basic implementation of our method, we use direct inversion (Gaussian elimination). Once the data-set $\{\omega_k\}$ is known, $f(z_a, t)$ is determined by a single $\mathcal{O}(N)$ numerical quadrature using (31). Thus, in an optimal implementation, determination of $f(z_a, t)$ is an $\mathcal{O}(N)$ procedure.

Our choice of parametrizing in arclength effectively places a practical restriction on the domains which we can treat here to those which have sufficiently smooth boundaries. Initial conditions possessing isolated points with very high curvature must be avoided because, for accurate solution of the S–L equation, a large value of N would be required to adequately resolve the neighbourhood of such points. It must be emphasized that this is purely a restriction imposed by our current implementation, and *not* an inherent restriction on the method. More sophisticated choices of parametrization will be implemented in future manifestations of the code and will enable effective calculation of the evolution of initial configurations close to an array of touching circular discs. Here, initial conditions are chosen in which the high curvature regions typical of such configurations of touching disks have been smoothed out slightly. Physically, this corresponds to avoiding the very early stages of sintering which is consistent with the fact that we only expect the isolated unit cell to model accurately pore shrinkage in the doubly-infinite lattice when the pore sizes are sufficiently small (compared to the area of the unit cell) and the effect of neighbouring cells not significant.

Figure 3 shows snapshots of Hopper's solution calculated using (27) and (28) with $f(z_a, t)$ computed using the S–L equation. A valuable check on the numerical solution of the S.L. equation is provided by comparison with the conformal-map solution.

7. A doubly-connected fluid domain

Now consider the unit problem consisting of four equal touching particles shown in Figure 1. The sintering of this domain was computed numerically by Van der Vorst [11] and later analytically by Richardson [9] and Crowdy [10] (who each used rather different formulations involving conformal maps). We now present the new algebraic-curve approach.

The mean-value theorem and additivity over the domain of disconnected disks implies that the associated quadrature identity is

$$\iint_{D(0)} h(z)\,\mathrm{d}x\,\mathrm{d}y = \pi r_1^2 h(z_1) + \pi r_2^2 h(z_2) + \pi r_3^2 h(z_3) + \pi r_4^2 h(z_4), \tag{33}$$

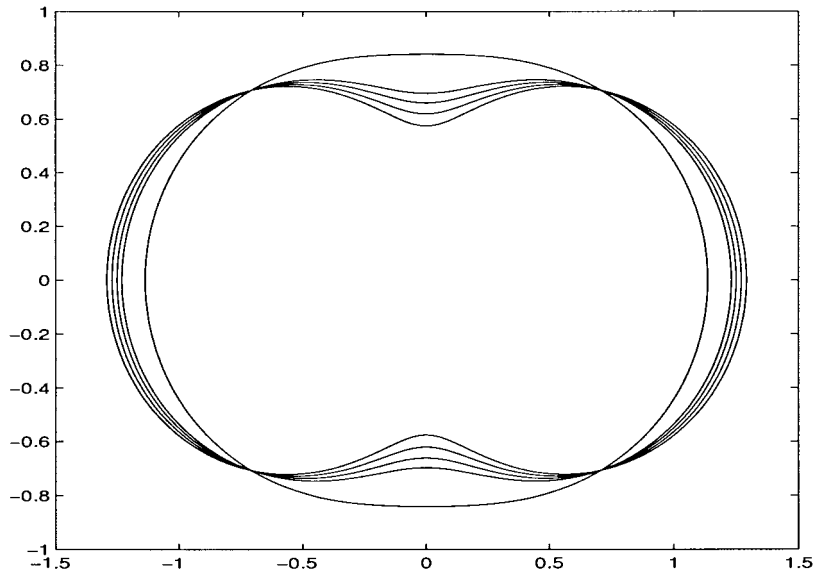

Figure 3. Hopper's solution calculated using algebraic curve approach. Figure shows superposed time sequence of algebraic curves $z^2\bar{z}^2 - z_a^2 z^2 - z_a^2\bar{z}^2 - 2r^2 z\bar{z} = 0$ with parameters $z_a, (t)$ and $r(t)$ satisfying the o.d.e.'s $\dot{z}_a = -2f(z_a, t)$ and $\dot{r} = 0$ with initial conditions $r(0) = \sqrt{0{\cdot}5}$ and $z_a(0) = 0{\cdot}6$. $f(z_a, t)$ is computed using the solution of Sherman-Lauricella integral equation; times shown $t = 0{\cdot}0, 0{\cdot}1, 0{\cdot}2, 0{\cdot}3, 0{\cdot}4, 1{\cdot}0$.

where

$$\begin{aligned} &r_1(0) = r_2(0) = r_3(0) = r_4(0) = 1; \\ &z_1(0) = \sqrt{2}; \qquad z_2(0) = i\sqrt{2}; \qquad z_3(0) = i\sqrt{2}; \qquad z_4(0) = -\mathrm{i}\sqrt{2}. \end{aligned} \tag{34}$$

and $h(z)$ is an arbitrary single-valued analytic function integrable over the domain. The associated algebraic curve is also easily found to be

$$\begin{aligned} \mathcal{P}(z, \bar{z}) &= (|z - z_1|^2 - 1)(|z - z_2|^2 - 1)(|z - z_3|^2 - 1)(|z - z_4|^2 - 1) \\ &= z^4\bar{z}^4 - z_1^4 z^4 - z_1^4\bar{z}^4 - 4r^2 z^3\bar{z}^3 + ez^2\bar{z}^2 + fz\bar{z} + k \\ &= 0, \end{aligned} \tag{35}$$

where

$$r = 1; \qquad e = 2; \qquad f = -4; \qquad k = 1. \tag{36}$$

From Crowdy [12], the evolution equations for the quadrature data in (33) is given by

$$\begin{aligned} &\dot{r}_j = 0, \quad j = 1, 2, 3, 4, \\ &\dot{z}_j = -2f(z_j, t), \quad j = 1, 2, 3, 4. \end{aligned} \tag{37}$$

There are four constants of the motion, and four time-evolving parameters. It is convenient to note that the physical problem preserves the four-fold rotational symmetry and dictates that

$$z_2(t) = \mathrm{i}z_1(t); \qquad z_3(t) = -z_1(t); \qquad z_4(t) = -\mathrm{i}z_1(t); \tag{38}$$

therefore, it is enough to solve

$$\dot{z}_1 = -2f(z_1, t). \tag{39}$$

and take $r_1(t) = r_2(t) = r_3(t) = r_4(t) = r$.

Having thus updated the quadrature data at each instant, we can use Theorem 4.1 to update the last two columns (and rows) of the matrix $\mathbf{A}(t)$. Using Theorem 4.1 and the four-fold rotational symmetry of the domain, we deduce that

$$\mathbf{A}(t) = \begin{pmatrix} k & 0 & 0 & 0 & -z_1^4 \\ 0 & f & 0 & 0 & 0 \\ 0 & 0 & e & 0 & 0 \\ 0 & 0 & 0 & -4r^2 & 0 \\ -z_1^4 & 0 & 0 & 0 & 1 \end{pmatrix} \tag{40}$$

where r is a constant of the motion and $z_1(t)$ satisfies (39). The zeros in (40) are forced by the rotational symmetry. The original free-boundary problem is reduced to determining the evolution of the algebraic curve matrix $\mathbf{A}(t)$. It just remains to determine $e(t)$, $f(t)$ and $k(t)$.

The multiply-connected quadrature domains associated with a given (fixed) quadrature identity are not unique. In the present example it is expected that there will exist a one-parameter family of quadrature domains all satisfying (33) but each having enclosed pores of different area (see Gustafsson [17] for a more technical abstract discussion of this point). The evolution of the areas of the pores is given by the following theorem:

THEOREM 7.1 (Evolution of pore areas)

Let $A_i(t)$ denote the area, at time t, of the i-th enclosed pore of a sinter body satisfying the initial conditions of Theorem 5.1. Then, under the viscous-sintering dynamics,

$$\dot{A}_i(t) = \frac{1}{2\mathrm{i}} \oint_{\partial D_i(t)} 2g'(z, t)\, \mathrm{d}z. \tag{41}$$

where $g'(z, t)$ is the Goursat function of Section 2.

Proof: If it is observed that

$$A_i(t) = \frac{1}{2\mathrm{i}} \oint_{\partial D_i(t)} \bar{z}\, \mathrm{d}z, \tag{42}$$

the result follows by taking the time-derivative of the right-hand side of (42) and making use of the boundary conditions in the same spirit as the proof of Theorem 3.1 of Crowdy [12]. We omit the details.

Recall that $g'(z, t)$ is determined from the solution of the S–L equation. It can be shown that, like $\dot{z}_1$, $\dot{A}_i(t)$ is determined by a single $\mathcal{O}(N_i)$ quadrature involving the S–L solution $\{\omega_k\}$. If the evolution of the pore area $A_1(t)$ provides an implicit evolution equation for $e(t)$, then two additional nonlinear equations for $f(t)$ and $k(t)$ (the analogues of (29)) are

$$\mathcal{F}_j(f, k) = 0,\ j = 1, 2, \tag{43}$$

where

$$\mathcal{F}_j(f,k) \equiv \frac{1}{2\mathrm{i}} \oint_{\partial D(t)} \mathrm{e}^{jz}\bar{z}dz - \pi r^2(2\cosh jz_1 + 2\cos jz_1), \quad j = 1, 2, \tag{44}$$

which result from taking the (arbitrary) linearly independent choices $h(z) = \mathrm{e}^z$ and $h(z) = \mathrm{e}^{2z}$ in (33) and using Green's theorem. As in Hopper's example, it turns out that Equations (43) can be replaced by a more convenient set by exploiting the special points V_0. The reader is referred to Crowdy [19] for more details.

To update the matrix $\mathbf{A}(t)$, 100 points are used in the discretization of both outer and inner contours in the first quadrant (it is enough, by symmetry, to consider the contours in this quadrant) and a simple forward Euler scheme (with time-step 0·01) is used to integrate the ordinary differential equations. A relatively smooth initial domain is chosen to ensure accuracy in solving the S–L equation and to avoid any stiffness problems associated with localized points of high curvature. In solving the S–L equation, the generalized representations for $f(z,t)$ and $g'(z,t)$ presented by Greengard, Kropinski and Mayo [21] for multiply-connected domains are used. In particular, because $f(z,t)$ is known to be single-valued, we continue to use the representation, (31) while simple pole singularities in each of the holes must be added to the representation of $g'(z,t)$ to account for the sources/sinks expected to be found therein.

It is again possible to check the evolution in this case by comparison with a conformal-mapping approach. Figure 4 shows both the evolution plotted using the loxodromic-function conformal map from a concentric annulus constructed in Crowdy [10] based on the theory of Crowdy and Tanveer [8], (although, if preferred, one could equivalently use an elliptic function conformal map from a rectangle as constructed by Richardson [9]) as well as the same solution calculated using the algebraic curve method. The curves show excellent agreement to within the numerical errors of the separate calculations. In both calculations, the enclosed pore is observed to shrink to a point just after $t = 0{\cdot}5$ (the last contour shown in Figure 4).

8. A quintuply-connected fluid domain

Surprisingly little additional effort is required to compute the evolution of the *quintuply*-connected domain relevant to the unit problem in Figure 2 discussed earlier. This calculation is new. The domain again has a four-fold rotational symmetry about the origin but now the additional central particle adds a single term to the quadrature identity of Section 7:

$$\iint_{D(0)} h(z)\mathrm{d}x\mathrm{d}y = \pi r_1^2 h(z_1) + \pi r_2^2 h(z_2) + \pi r_3^2 h(z_3) + \pi r_4^2 h(z_4) + \pi p^2 h(z_0), \tag{45}$$

where

$$z_0(0) = 0, \quad z_1(0) = \sqrt{2}, \quad z_2(0) = \mathrm{i}\sqrt{2}, \quad z_3(0) = -\sqrt{2}, \quad z_4(0) = -\mathrm{i}\sqrt{2}, \tag{46}$$

and

$$r_1(0) = r_2(0) = r_3(0) = r_4(0) = 1; \qquad p(0) = \sqrt{2} - 1. \tag{47}$$

The quadrature identity now has order 5. By Theorem 5.1 the domain $D(t)$ continues to satisfy (45) under evolution with quadrature data satisfying the o.d.e.'s

$$\begin{aligned} \dot{p} &= 0; \qquad \dot{z}_0(t) &&= -2f(z_0,t); \\ \dot{r}_j &= 0; \qquad \dot{z}_j(t) &&= -2f(z_j,t), k = 1, \ldots, 4. \end{aligned} \tag{48}$$

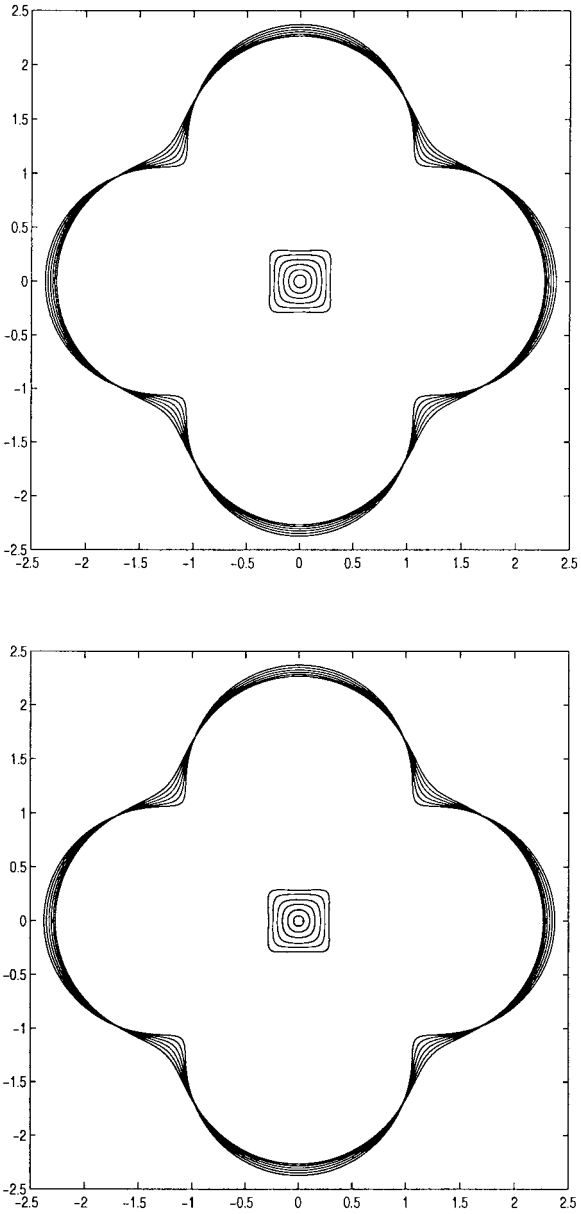

Figure 4. Evolution of the unit problem derived from the lattice in Figure 1. Calculation is performed up to point where enclosed pore is about to vanish. Upper diagram shows evolution computed using conformal map of [8] [10]; lower diagram shows the same calculation performed using algebraic curve parametrization. Times shown in both figures are $t = 0{\cdot}0, 0{\cdot}1, 0{\cdot}2, 0{\cdot}3, 0{\cdot}4, 0{\cdot}5$.

The rotational symmetry forces $f(0,t) = 0$ so that $z_0(t) = 0$ and it is again enough to integrate the single ordinary differential equation

$$\dot{z}_1 = -2f(z_1, t). \tag{49}$$

Using Theorem 4.1 and the symmetry of the domain, we deduce that the associated matrix $\mathbf{A}(t)$ is given by

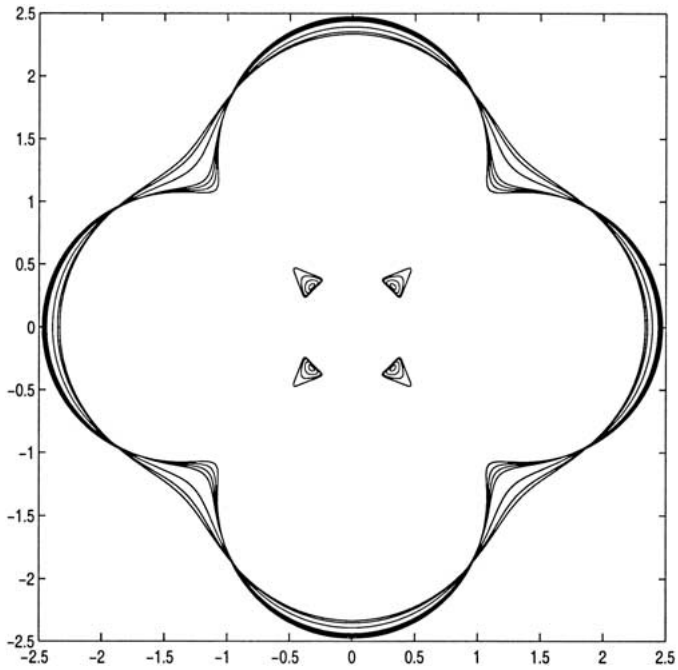

Figure 5. Pore shrinkage in a quintuply connected sinter body with four enclosed pores. The unit problem derives from the lattice in Figure 2. Calculation is performed by tracking the evolution of the five real parameters $z_1(t), e(t), f(t), k(t)$ and $l(t)$ in the algebraic curve matrix $\mathbf{A}(t)$. Times shown are $t = 0{\cdot}0, 0{\cdot}05, 0{\cdot}1, 0{\cdot}15, 0{\cdot}4, 0{\cdot}65$ and $0{\cdot}775$. By $t = 0{\cdot}15$ pores have almost disappeared, but the same algebraic curve is still valid even after pores have vanished.

$$\mathbf{A}(t) = \begin{pmatrix} l & 0 & 0 & 0 & z_1^4 p^2 & 0 \\ 0 & k & 0 & 0 & 0 & -z_1^4 \\ 0 & 0 & f & 0 & 0 & 0 \\ 0 & 0 & 0 & e & 0 & 0 \\ z_1^4 p^2 & 0 & 0 & 0 & -(4r^2 + p^2) & 0 \\ 0 & -z_1^4 & 0 & 0 & 0 & 1 \end{pmatrix}. \tag{50}$$

The zeros in (50) are again forced by the rotational symmetry. The initial disconnected domain of touching circles corresponds to the parameter set

$$\begin{aligned} &r(0) = 1; \qquad p(0) = \sqrt{2} - 1; \quad e(0) = 10 - 8\sqrt{2}; \\ &f(0) = 2 - 4\sqrt{2}; \;\; k(0) = 13 - 8\sqrt{2}; \;\; l(0) = -3 + 2\sqrt{2}. \end{aligned} \tag{51}$$

The free-boundary problem has thus been reduced to finding the evolution of the matrix $\mathbf{A}(t)$. This is done using precisely the same technology developed in previous examples.

Figure 5 shows an example in which the four enclosed pores shrink until they vanish - by $t = 0{\cdot}15$ all the pores have almost disappeared; however the calculation has been continued up to $t = 0{\cdot}775$. This highlights one of the benefits of our method. Once the pores have become negligibly small, the algebraic curve description of the fluid boundary is *still* valid; the vanishing of the pores simply corresponds to the algebraic curve $\mathcal{P}(x + \mathrm{i}y, x - \mathrm{i}y; t) = 0$

having fewer solutions for real x and y than it did before the pores vanished. A conformal-map approach would become singular at such a pore-shrink-age event; it would be necessary to switch to a different functional form of conformal map from a different canonical parametric region. The approach above avoids these topological complications.

It is of interest to observe from the shapes of the enclosed pores in Figure 5 that, during the early part of the calculation, the neck radii between equal-sized particles grows quickly, while the necks between unequal particles only grow significantly once the 'equal neck' regions have become sufficiently large. While Van der Vorst [11] pointed out the usefulness of considering simple unit problems in the study of sintering, this observation highlights the limitations in satisfactorily employing simple unit problems (such as Hopper's coalescence result for equal particles [4] or Richardson's [6] result for unequal particles) to deduce quantitative information on densification in any but the most simple sinter compacts. Figure 5 suggests that the sintering of the four surrounding equal particles is exerting stresses that impedes the coalescence of the different-sized particles. Scherer [22] has similarly discussed the effects that a bimodal distribution of particles can have on the global densification by giving rise to differentials in sintering stresses throughout the sinter body. We intend to examine such issues, based on the exact solution methods presented here, in more detail in future work. It is also necessary to investigate in future work the effect of considering this quintuply-connected unit problem isolated from the rest of the doubly-infinite lattice (*cf.* [13]).

9. Discussion

The initial domains relevant to planar viscous sintering are usually configurations of touching circular disks modelling a configuration of touching particles [4–6],[9–11]. Such domains are quadrature domains with boundaries that are algebraic curves which, moreover, can often be written down immediately from simple geometrical considerations. With enough symmetry in the configuration, it has been shown here that the evolution preserves the form of this algebraic curve and it is natural to compute the subsequent sintering dynamics of such configurations by tracking the evolution of this curve. This paper has proposed, and implemented, this strategy.

An alternative method is to construct the uniformization maps of these algebraic curves; this is essentially equivalent to the traditional conformal-mapping approach to the problem and results of this kind have currently only been computed for the simply and doubly-connected sintering problems. In principle, uniformization maps can be constructed for quadrature-domain fluid regions of any finite connectivity. While a conformal map has the advantage of being an *explicit* representation of the fluid boundary, there is much analytical overhead required to construct, say, the uniformization of the algebraic curve (50) which, in the case where it describes a quintuply-connected fluid region, is associated with a compact genus-4 Riemann surface (the conformal map could be constructed as an automorphic function on the universal cover of this Riemann surface). Even with this done, the evolution of the conformal-mapping parameters will require the solution, at each instant, of a finite set of nonlinear equations, some of which depend non-locally on the domain. But nothing more than this is required to determine the evolution of the finite set of algebraic-curve parameters. In addition, it has been seen that the algebraic curve approach has the advantage of coping automatically with reduction in connectivity (physically, pore shrinkage - a ubiquitous event in the current application). The *conceptual* simplicity of the algebraic-curve approach only adds further to its practical appeal.

It is worth emphasizing the advantages of our approach over a purely numerical scheme based on boundary-integral methods [23], [24], [11], where N points on the boundary would be time-advanced individually. Indeed, in solving the S-L equation, we have essentially used ideas normally employed in the context of boundary-integral calculations. The important point is that we have identified, and are exploiting, a *finite* representation of the fluid boundary valid at all times in the evolution. The solution at any stage of sintering requires only the determination of a (usually small) finite set of parameters and the state of the fluid boundary can be reported in finite (usually C^∞) form. Moreover, knowledge of a closed-form algebraic formula for the curve is crucial in facilitating quick-and-easy solution of the S-L equation and provides closed form formulae for the tangent and curvature at any point on the curve and at all times during the calculation. The finite representation of the boundary also reduces memory requirements.

Crowdy [19] has made use of analytical properties of the special points of quadrature domains to simplify the numerical construction of the domains when there exists sufficient symmetry in the problem; but the viscous-sintering problem only admits exact quadrature-domain solutions when the domains *do* have such symmetry! Moreover, as has been seen here, many interesting sintering scenarios fall within this class. The exploitation of special points in the construction of symmetric quadrature domains is therefore valuable in this physical application. There remain further questions as to whether advances in the understanding of the linear analysis of quadrature domains [25] can further simplify computations of viscous sintering.

Recent calculations [10] of doubly-connected fluid domains that use exact solutions based on conformal maps reveal that the planar sintering problem, while physically simplistic, shares many *qualitative* features with the fully three-dimensional problem. Furthermore, Nie and Tanveer [26] have studied the *axisymmetric* sintering problem numerically and found that it shares many behavioural features with the planar problem. This evidence, coupled with its various mathematical properties, render the planar sintering problem a useful and analytically tractable theoretical paradigm. In an optimal implementation, our approach provides a fast, flexible and versatile method to compute the evolution of a wide range of planar unit problems, the behavioural characteristics of which can be studied in detail and any qualitative results potentially extrapolated to the (much less tractable) three-dimensional problem. We believe the approach represents a practical middle ground between the concise, predominantly analytical, solutions of Hopper [4] on the one hand, and purely numerical calculations *e.g.* Kuiken [23, 24], Van der Vorst [13], [11], [27], Primo *et al.* [28]) on the other.

Acknowledgements

The author acknowledges many useful discussions with Professor S. Tanveer of Ohio State University. The author also acknowledges financial support from the Nuffield Foundation and EPSRC (GR/R40104/01).

References

1. C.J. Brinker and G.W. Scherer, *Sol-Gel Science.* Boston: Academic Press Inc (1990) 908pp.
2. J. Frenkel, Viscous flow of crystalline bodies under the action of surface tension. *J. Phys. (Moscow)* 9 (1945) 385–391.

3. J.K. Mackenzie and R. Shuttleworth, Phenomenological theory of sintering. *Proc. Phys. Soc. London* 62 (1949) 833–852.
4. R.W. Hopper, Coalescence of two equal cylinders: exact results for creeping viscous flow driven by capillarity. *J. Am. Ceram. Soc.* 67 (1985) C262–264.
5. R.W. Hopper, Plane Stokes flow driven by capillarity on a free surface. *J. Fluid Mech* 213 (1990) 349–375.
6. S. Richardson, Two-dimensional slow viscous flows with time-dependent free boundaries driven by surface tension. *Eur. J. Appl. Math* 3 (1992) 193–207.
7. S.D. Howison, www.maths.ox.ac.uk/howison/Hele-Shaw.
8. D.G. Crowdy and S. Tanveer, A theory of exact solutions for annular viscous blobs. *J. Nonlinear Sci* 8 (1998) 375–400 and Erratum. *J. Nonlin. Sci* 11 (2001) 237.
9. S. Richardson, Plane Stokes flow with time-dependent free boundaries in which the fluid occupies a doubly-connected region. *Eur. J. Appl. Math* 11 (2000) 249–269.
10. D.G. Crowdy, Viscous sintering of unimodal and bimodal cylindrical packings with shrinking pores. *Eur. J. Appl. Math* (submitted).
11. G.A.L. Van de Vorst, Integral method for a two-dimensional Stokes flow with shrinking holes applied to viscous sintering. *J. Fluid Mech.* 257 (1993) 667–689.
12. D.G. Crowdy, A note on viscous sintering and quadrature identities. *Eur. J. Appl. Math.* 10 (1999) 623–634.
13. G.A.L. Van de Vorst, Integral formulation to simulate the viscous sintering of a two-dimensional lattice of periodic unit cells. *J. Eng. Math.* 30 (1996) 97–118.
14. D.G. Crowdy and S. Tanveer, A theory of exact solutions for plane viscous blobs. *J. Nonlinear Sci.* 8 (1998) 261–279.
15. S. Richardson, Two-dimensional bubbles in slow viscous flows. *J. Fluid Mech.* 33 (1968) 475–493.
16. D. Aharonov and H. Shapiro, Domains on which analytic functions satisfy quadrature identities. *J. Anal. Math.* 30 (1976) 39–73.
17. B. Gustafsson, Quadrature identities and the Schottky double. *Acta. Appl. Math.* 1 (1983) 2O9–240.
18. D.G. Crowdy, On a class of geometry-driven free boundary problems. *SIAM J. Appl. Math.* 62 (2002) 945–964.
19. D.G. Crowdy, On the construction of multiply-connected quadrature domains. *SIAM J. Appl. Math.* (2002) to appear.
20. A. Greenbaum, L. Greengard and A. Mayo, On the numerical solution of the biharmonic equation in the plane. *Physica D* 60 (1992) 216–225.
21. L. Greengard, M.C. Kropinski and A. Mayo, Integral equation methods for Stokes flow and isotropic elasticity in the plane. *J. Comp. Phys.* 125 (1996) 403–414.
22. G.W. Scherer, Viscous sintering of a bimodal pore-size distribution. *J. Am. Ceram. Soc.* 67 (1984) 709J715.
23. H.K. Kuiken, Viscous sintering: the surface-tension-driven flow of a liquid form under the influence of curvature gradients at its surface. *J. Fluid Mech.* 214 (1990) 503–515.
24. H.K. Kuiken, Deforming surfaces and viscous sintering. In: D.G. Dritschel and R.J. Perkins (eds.), *The Mathematics of Deforming Surfaces.* Oxford: Clarendon Press (1996) pp. 75–91.
25. M. Putinar, Linear analysis of quadrature domains. *Ark. Mat.* 33 (1995) 357–376.
26. Q. Nie and S. Tanveer, (private communication).
27. G.A.L. Van de Vorst, Integral formulation to simulate the viscous sinter. of a two-dimensional lattice of periodic unit cells. *J. Eng. Math.* 30 (1996) 97–118.
28. A.R.M. Primo, L.C. Wrobel and H. Power, An indirect boundary-element method for slow viscous flow in a bounded region containing air bubbles. *J. Eng. Math.* 37 (2000) 305–326.